

# Epitaxial ZrSe<sub>2</sub>/MoSe<sub>2</sub> semiconductor v.d. Waals heterostructures on wide band gap AlN substrates



P. Tsipas<sup>a</sup>, D. Tsoutsou<sup>a</sup>, J. Marquez-Velasco<sup>a</sup>, K.E. Aretouli<sup>a,b</sup>, E. Xenogiannopoulou<sup>a</sup>, E. Vassalou<sup>a</sup>, G. Kordas<sup>a</sup>, A. Dimoulas<sup>a,\*</sup>

<sup>a</sup> Institute of Nanoscience and Nanotechnology, NCSR DEMOKRITOS, 15310 Athens, Greece

<sup>b</sup> University of Athens, Department of Physics, Section of Solid State Physics, 15684 Athens, Greece

## ARTICLE INFO

### Article history:

Received 23 February 2015

Received in revised form 19 March 2015

Accepted 10 April 2015

Available online 29 April 2015

### Keywords:

MBE

2D semiconductors

ZrSe<sub>2</sub> films

ZrSe<sub>2</sub>/MoSe<sub>2</sub> heterostructures

Band alignment

Band structure

## ABSTRACT

Using molecular beam epitaxy (MBE) of ZrSe<sub>2</sub> and ZrSe<sub>2</sub>/MoSe<sub>2</sub> heterostructures are grown on crystalline AlN(0001)/Si(111) substrates. Electron diffraction (RHEED) and valence band imaging by angle resolved photoelectron spectroscopy (ARPES) indicate high quality heteroepitaxial growth with very good in-plane crystallographic alignment with the substrate. The workfunction and band offsets are estimated by photoelectron spectroscopy and compared with first principles calculations. The constructed band alignments show that the heterostructure could form the basis for atomically thin p–n junction and 2D vertical tunneling devices.

© 2015 Elsevier B.V. All rights reserved.

## 1. Introduction

Atomically thin group VIB dichalcogenide ((Mo, W)X<sub>2</sub>) 2D semiconductors have been extensively studied showing great potential to impact nanoelectronics. Moreover, VIB/VIB dichalcogenide heterostructures and p–n junctions [1–3] have been recently demonstrated. On the other hand, alternative group IVB dichalcogenides (e.g. ZrSe<sub>2</sub>, HfSe<sub>2</sub>) remain unexplored. Due to van der Waals heteroepitaxy [4] and the variety of energy gaps and electron affinities, VIB/IVB dichalcogenide heterostructures offer the possibility of sharp, defect-free heterointerfaces with type-II or type-III band alignments [5] and with potential applications in vertical staggered or broken gap 2D TFETs [6]. MBE-grown HfSe<sub>2</sub> on HOPG and exfoliated MoS<sub>2</sub> have been recently reported [7]. In another work, HfSe<sub>2</sub> and MoSe<sub>2</sub>/HfSe<sub>2</sub> on crystalline AlN substrates are studied [8].

In this work, we report epitaxial ZrSe<sub>2</sub> and ZrSe<sub>2</sub>/MoSe<sub>2</sub> heterostructures on wide band gap AlN(0001)/Si(111) substrates offering the benefits of a semiconductor-on-insulator approach. Since AlN/Si substrates are readily available in 300 mm wafer sizes, they offer a manufacturable route for 2D semiconductor volume

production in-line with industry's wafer size and processing standards. We employ structural and physical characterization as well as first principles to verify the quality of our films while the band alignment of the two dichalcogenide films is determined.

## 2. Experimental and computational details

The 2D semiconductors are grown in an Ultra-High Vacuum (UHV) chamber by MBE on MOCVD-grown 200 nm AlN(0001)/Si(111) substrates. Details about the surface preparation of the AlN substrates are given elsewhere [9]. High purity Mo (99.95%) and Zr (99.95%) are evaporated by e-beam and Se (99.999%) from an effusion cell with Se/metal overpressure of ~15:1. First, ZrSe<sub>2</sub> films are grown directly on AlN with thicknesses in the range of 1–10 monolayers (ML). A two-step growth is employed, first at 590 °C, followed by in situ, UHV annealing at 810 °C to improve crystallinity. In another set of samples, ZrSe<sub>2</sub> films are grown on MoSe<sub>2</sub>/AlN structures. In this case, ZrSe<sub>2</sub> film growth and UHV annealing procedures are performed at 350 °C and 690 °C, respectively. The whole growth procedure is monitored by in situ Reflection High Energy Electron Diffraction (RHEED). After growth, the samples are transferred in a UHV chamber without being exposed to ambient for X-ray Photoelectron Spectroscopy (XPS), Ultraviolet Photoelectron Spectroscopy (UPS) and Angle-Resolved Photoemission Spectroscopy (ARPES) measurements in order to derive films stoichiometry, workfunction, band alignments and

\* Corresponding author at: National Center for Scientific Research "Demokritos", Patriarchou Gregoriou & Neapoleos, 15310 Agia Paraskevi, Attiki, Greece. Tel.: +30 210 6503340.

E-mail address: [a.dimoulas@inn.demokritos.gr](mailto:a.dimoulas@inn.demokritos.gr) (A. Dimoulas).

band structure. Raman spectroscopy complements the characterization of ZrSe<sub>2</sub> layers.

The calculations are performed within the density functional theory (DFT) framework by using the Vienna ab initio simulation package [10]. The Perdew–Burke–Ernzerhof (PBE) exchange–correlation functional [11] is engaged for our calculations with a plane-wave cutoff of 250 eV and a (21 × 21 × 1) *k*-point mesh. van der Waals interactions are taken into account through a dispersion correction as proposed by Grimme (DFT-D3 method) [12]. All the atoms are allowed to relax until the force and the energy are converged to 10<sup>−4</sup> eV/Å and 5 × 10<sup>−5</sup> eV, respectively. More than 25 Å of vacuum is included to ensure the isolation of the two sides of the slab.

### 3. Results and discussion

Fig. 1(a) shows the RHEED patterns of ZrSe<sub>2</sub> films directly grown on AlN substrates at several thicknesses. A perfect alignment of the two lattices is observed and the overall streaky pattern shows that ZrSe<sub>2</sub> grows epitaxially on the AlN substrates without any evidence for 3D growth or rough surfaces. RHEED patterns of bare AlN, MoSe<sub>2</sub> and ZrSe<sub>2</sub> films are shown in Fig. 1(b). From these patterns we can conclude that both dichalcogenide films grow epitaxially such that the [1–120] crystallographic direction is aligned in-plane with the same direction in the AlN substrate. The position of the diffraction streaks correspond to bulk-like lattice constants of AlN (3.10 Å), MoSe<sub>2</sub> (3.29 Å) and ZrSe<sub>2</sub> (3.77 Å), indicating that despite the appreciable lattice mismatch, the overgrown semiconductor films adopt their bulk lattice constant values as it would be expected for van der Waals heteroepitaxy. The streaky pattern of Fig. 1(b) indicates smooth surfaces for both epitaxial films, MoSe<sub>2</sub> and ZrSe<sub>2</sub>. Diffraction streaks from rotational domains are not observed indicating well-oriented epilayers in single-crystal form.

Fig. 2 shows the Raman spectra for a 10 ML ZrSe<sub>2</sub> film where two active modes are observed, namely the A<sub>1g</sub> and E<sub>g</sub> modes.

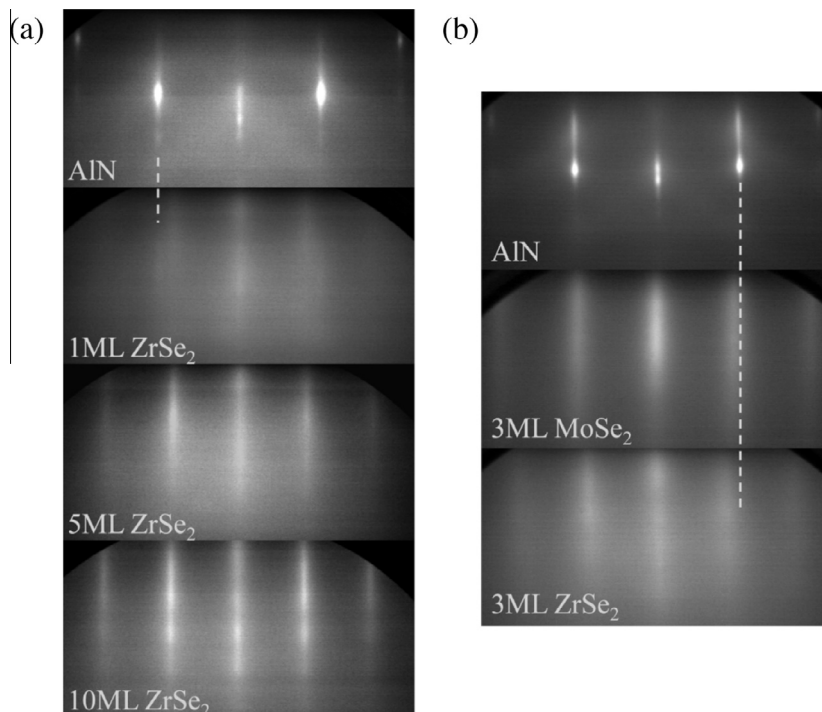


Fig. 1. (a) RHEED diffraction patterns of bare AlN(0001), 1 ML, 5 ML and 10 ML ZrSe<sub>2</sub> films along the [1–120] azimuth of AlN. (b) RHEED patterns of bare AlN(0001), 2 ML MoSe<sub>2</sub> and 3 ML ZrSe<sub>2</sub> films. A perfect alignment of the three lattices is observed.

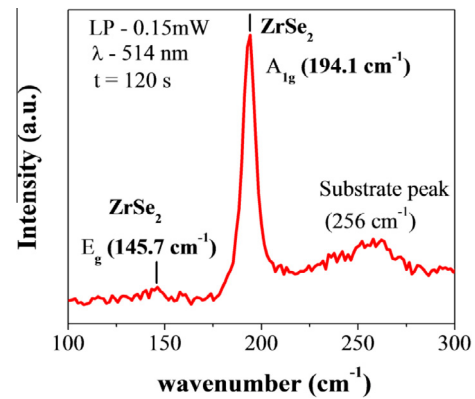


Fig. 2. Raman spectra of a 10 ML ZrSe<sub>2</sub> film. Raman peaks occur at 145.7 cm<sup>−1</sup> and 194.1 cm<sup>−1</sup> and can be assigned to the E<sub>g</sub> and A<sub>1g</sub> modes, respectively. The power and the wavelength of laser source are 0.15 mW and 514 nm, respectively, while the exposition time is 120 s.

The phonon frequencies of these two modes are determined as 194.1 cm<sup>−1</sup> and 145.7 cm<sup>−1</sup>, respectively, in good agreement with bulk crystals [13]. Mapping over large areas on the sample size of 1.7 cm × 1.7 cm show little or no variation of the Raman peaks with respect to Raman shift, intensity and linewidth, indicating very good uniformity continuous films.

The electronic valence band (VB) structure of 3 ML ZrSe<sub>2</sub> is imaged by in situ ARPES (Fig. 3(a)) recorded with a Helium I (HeI) photon line (h·ν = 21.22 eV) and compared with DFT band structure calculations (Fig. 3(b)) obtained using GGA–van der Waals potentials. The results show a good agreement of VB energy dispersions along the *Γ*M crystallographic direction between experiment and theory, the latter indicating an indirect gap of 0.65 eV (Fig. 3(b)). Since the Fermi level is located inside the gap, it is not possible to detect the conduction band and measure the

Download English Version:

<https://daneshyari.com/en/article/6943026>

Download Persian Version:

<https://daneshyari.com/article/6943026>

[Daneshyari.com](https://daneshyari.com)